Organic carbon fluxes of a glacier surface: a case study of Foxfonna, a small Arctic glacier

Short title: Organic carbon fluxes of an Arctic glacier surface

Krystyna A. Koziol[1,2,3*], Helen L. Moggridge[1], Joseph M. Cook[1], Andy J. Hodson[3,4]

[1] Department of Geography, University of Sheffield, Winter Street, S10 2TN

[2] Department of Arctic Geophysics, University Centre in Svalbard, P.O. box 156, 9171 Longyearbyen, Norway

[3] *current affiliation*: Department of Analytical Chemistry, Chemical Faculty, Gdansk University of Technology, Narutowicza 11/12, 80-233 Gdansk, Poland

[4] University Centre in Svalbard, Department of Arctic Geology, P.O. box 156, 9171 Longyearbyen, Svalbard.

[5] Department of Environmental Sciences, Western Norway University of Applied Sciences, 6856 Sogndal, Norway.

* corresponding author; email: k.a.koziol[at]gmail.com

Abstract (252 words)

Arctic glaciers are rapidly responding to global warming by releasing organic carbon (OC) to downstream ecosystems. The glacier surface is arguably the most biologically active and biodiverse glacial habitat and therefore the site of important OC transformation and storage, although rates and magnitudes are poorly constrained. In this paper, we present measurements of OC fluxes associated with atmospheric deposition, ice melt, biological growth, fluvial transport and storage (in superimposed ice and cryoconite debris) for a supraglacial catchment on Foxfonna glacier, Svalbard (Norway), across two consecutive years. We found that in general atmospheric OC input (averaging 0.63 ± 0.25 Mg a^{-1} total organic carbon, i.e. TOC, and 0.40 ± 0.22 Mg a^{-1} dissolved organic carbon, i.e. DOC) exceeded fluvial OC export (0.46 ± 0.04 Mg a^{-1} TOC and 0.36 ± 0.03 Mg a^{-1} DOC). Early in the summer, OC was mobilised in snowmelt but its release was delayed by temporary storage in superimposed ice on the glacier surface. This delayed the export of 28.5% of the TOC in runoff. Biological production in cryoconite deposits was a negligible potential source of OC to runoff, whilst englacial ice melt was far more important on account of the glacier's negative ice mass balance (-0.89 and -0.42 m a^{-1} in 2011 and 2012, respectively). However, construction of a detailed OC budget using these fluxes shows an excess of inputs over outputs, resulting in a net retention of OC on the glacier surface at a rate that would require *c.* 3 years to account for the OC stored as cryoconite debris.

Introduction

Arctic and mountain glaciers store organic carbon (OC) in dissolved and particulate forms. OC originates from recent and past incorporation into the glacial system, and encompasses both the ancient organic matter from fossil fuels (Stubbins et al., 2012) and the OC currently supplied by active microbial ecosystems (Anesio et al., 2009; Hodson et al., 2008). This OC, especially its dark particulate forms, is most likely contributing to the darkening of glacier surfaces (Cook et al., 2017; Takeuchi et al., 2001; Xu et al., 2012). Climate warming has accelerated the melting of Arctic glaciers (Gardner et al., 2011; Moholdt et al., 2010) and such darkening amplifies this process through the 'bioalbedo' effect (Bøggild et al., 2010; Cook et al., 2017; Takeuchi et al., 2014). Glacier shrinkage leads to greater OC fluxes reaching downstream ecosystems: Hood et al. (2015) estimate such an increase in glacial dissolved OC (DOC) flux for 13%. The main source of this increased DOC release are currently mountain glaciers, which makes their bioavailable OC cycles arguably the most rapidly changing amongst glaciers. OC in those is deemed predominantly allochthonous (Singer et al., 2012; Stibal et al., 2008; Xu et al., 2013). Therefore, the inputs and outputs of OC in such systems depend on the physical processes in the glacier system, and are at least partially climate-driven (by air temperature, precipitation, wind speed and direction changes). However, the link remains poorly defined due to lack of detailed field studies in constrained systems which would incorporate a mass balance scheme to reflect these climate-driven changes.

The work in this field to date comprises several studies which have examined carbon fluxes and storage on ice surfaces (e.g. Chandler et al., 2015; Cook et al., 2010, 2012; Hodson et al., 2010a; Musilova et al., 2017; Stibal et al., 2010, 2012b; Takeuchi, 2002). Further articles report regional or global estimations of OC release

from glaciers (Bhatia et al., 2013; Hood et al., 2015; Liu et al., 2016). Table 1 reports the main findings of such studies, the flux estimates, mainly for OC deposition in snow, removal in runoff and storage within glacial ice. However, due to lack of field-based data, none of these studies has incorporated summer precipitation or dust deposition. Furthermore, in order to consider the role of the darkening glacier surfaces in altering glacial OC cycles, the melt release from englacial storage and runoff removal from the glacier surface need to be treated as separate terms, with the supraglacial OC storage as an intermediate stage. Such supraglacial OC storage requires an appreciation of the autochthonous as well as the allochthonous inputs of OC from a range of sources (Stibal et al, 2006) and their likely biological transformation within snow and glacier ice (Stibal et al., 2012a). Therefore, we aimed in this paper to add those usually missing fluxes to the OC cycle study, and to integrate OC inputs, storage and release with a mass balance scheme. By expanding the typical scope of glacial OC fluxes considered, we intended to link the supraglacial carbon cycle to the physical features of the glacial system, with its spatial and temporal variability. As a result, we make a crucial step towards understanding the role played by the supraglacial environment in the overall glacial carbon exchange, and thus also predicting the glacial carbon cycle reaction to climate warming.

These elements were included in a conceptual model for the organic carbon mass balance of a hypothetical glacier (Figure 1). In this paper we quantified these terms for Foxfonna glacier, Svalbard (Norway), using data from two consecutive whole-summer field campaigns .

Materials and methods

Field site

The field site was on the cold-based Foxfonna glacier (Koziol, 2014; Liestøl, 1974), in Nordenskiöld Land, Svalbard (Norway; Fig. 2). A supraglacial catchment covering almost the entire elevation range of the glacier was instrumented (Fig. 3) between June and August in 2011 and 2012. Due to interannual variations in the timing of spring snowmelt, pre-melt snow sampling was carried out in April 2011 and June 2012. The surface area of the catchment varied only slightly between the investigated years, amounting to 1.27 km^2 in 2011 and 1.31 km^2 in 2012. Meteorological data (air temperature, relative humidity, wind speed, incident radiation) was measured at the local automatic weather station, however the nearest weather station measuring precipitation was 17.5 km away (WMO station at Svalbard Lufthavn).

The choice of a small, predominantly cold-based glacier is both beneficial and limiting. The data collected here refer to a certain class of glaciers, simpler to understand and representing the likely future for many current glacial systems. However, the OC flux scheme described there does not incorporate subglacial processes, calving and the pronounced autochthonous OC production in the interior of ice-sheets.

Atmospheric deposition (*A*)

Net atmospheric deposition *A* was calculated as the sum of deposition from "winter" (A^{acc}) and "summer" (A^{abl}) inputs (Equation 1). OC in the late winter snowpack was assumed to represent the sum of OC scavenged from the atmosphere and deposited directly by wet and dry deposition (*sensu* Schlesinger and Bernhardt, 2013) during

the winter snow accumulation period. OC in the late pre-melt snowpack was measured at 10 sites in 2011 and 14 sites in 2012 (Fig. 3). At each site a snow core was collected into a pre-cleaned plastic zip-lock sample bag and slowly melted in the dark. Sample aliquots of 50 mL were sealed in pre-rinsed centrifuge tubes and stored at -20°C for transport to the University of Sheffield (UK). These aliquots were then analysed using a Sievers 900 TOC analyser. At 5 sites the vertical distribution of OC in the snow cover was also studied by extracting samples from 4-6 samples from stratigraphic layers.

During the ablation season, there is frequent washaway of deposited OC, necessitating frequent sampling of atmospheric inputs using dust traps modified from Hall and Upton (1988) and Irvine-Fynn et al. (2012). Trap details are available in Supplementary Information. The atmospheric flux 'A' was then determined as:

(1) $A = A^{acc} + A^{abl}$.

Fluvial export (Qc)

Meltwater runoff was sampled every 2–3 days for most of the melt season on the proglacial stream (Site B1 on Fig. 1.). Every other measurement was accompanied by sampling the streams on the glacier snout (B2, B3 & B4 on Fig. 1.). All stream water samples were collected using pre-rinsed centrifuge tubes and frozen at -20°C for transport.

The proglacial stream (B1) water level was measured hourly using a Druck PDCR submersible pressure transducer, enabling discharge to be calculated. It was calibrated with salt dilution discharge gauging on 26 occasions in 2011 and 23 occasions in 2012 (multiple rating curves were used due to channel geometry change during the melt season). The relative standard errors (RSE) of the discharge estimates (Hodgkins, 2001) were 13.9% in 2011 and 18.9% in 2012.

Net glacier mass balance contribution (*Ic*)

The *Ic* term represents the loss of englacial OC (see Figure 1) via surface ablation. This was estimated from observations of glacier ice ablation and the spatially distributed OC content of glacier ice in six shallow cores (Fig. 3) collected at the end of summer 2011 using a stainless steel Kovacs ice auger. In each case, a 1-m deep glacier ice section was sampled at 20 cm intervals by collecting ice chips with clean, powder-free gloves. The drill was rinsed with 18 MΩ deionised water between and prior to sampling. The amount of glacier ice ablation was estimated from an annual net glacier mass balance survey conducted at ablation stakes A1–5 (Fig. 3) on 2nd September each year. The glacier-ice samples were processed and stored in the same manner as the snow samples.

Superimposed ice (*SI*)

In order to measure the maximum transient OC storage in superimposed ice, sampling coincided with its maximum observed thickness at the end of July (just prior to snow cover loss) in both years. Cores were collected from 9 locations in 2012, but just one location in 2011 (E7 in Fig. 3, where 3 cores were taken). Therefore, the 2011 estimate was scaled up using the ratio between deposition measured at this point and the spatial average of deposition in 2012. The samples were stored and processed following the protocol adopted for snow and glacial ice samples.

Biological production (*Δbio*)

Cryoconite debris on the glacier surface is by far the most biologically active microbial habitat on the glacier surface (Hodson et al., 2008). Net ecosystem production (*NEP*) and respiration (*R*) rates of cryoconite were therefore measured by

means of *in situ* 24 hour incubations of cryoconite following the methodology of Hodson et al. (2010b), using 300 mL sterile Whirlpak® bags as incubation vessels. Biological production (*Δbio*) was assumed to be equivalent to *NEP*, and the primary productivity (*PP*) was calculated from Equation 2, in order to facilitate comparison with other glacial ecosystem productivity studies:

(2) *Δbio = NEP = PP – R.*

Five sets of six incubations were prepared in 2011 and three sets of six incubations in 2012, using three locations at different elevations (A1, A2 and A4 in Fig. 3). Corrections for carbonate dissolution in all incubations were made following major cation determination using Dionex ICS-90 ion chromatography, and by assuming that increases in Ca^{2+} and Mg^{2+} concentrations during the incubations came solely from weathering of carbonates (Hodson et al., 2010b). Thus, the remaining inorganic carbon flux is assumed to equal the TOC flux here.

Δbio estimates are only presented as TOC fluxes here because the relative importance of DOC and POC (particulate organic carbon or biomass) in the *PP* or *R* fluxes was impossible to determine using the method adopted.

Storage in supraglacial debris (*SOC*)

Beneath the snow and superimposed ice, cryoconite was assumed to be the dominant supraglacial store of particulate OC, on account of there being no medial moraines. Cryoconite was systematically surveyed by photographing the glacier surface and collecting samples for quantifying OC at 24 locations at 200 m distance intervals (Fig. 3). At each location, ≥16 pictures were taken using a Sony DSLR-A390 digital camera with a fixed focal length and height above the ice surface (1 m), producing images of *c.* 0.145 m^2 (± 0.040, 1 SD). The survey was conducted at the

end of 2011 summer season, but was not repeated in 2012 due to early snowfall. Photos were processed using ImageJ software, following Irvine-Fynn et al. (2010), with a manual threshold selection to account for spatial differences in sediment hue. Once the areal extent of the cryoconite was determined, a transfer function was used to estimate the mass (see section *Flux calculations*).

Analytical procedure

Total organic carbon (TOC) and dissolved organic carbon (DOC) analysis were conducted on freshly melted samples using a Sievers 5310 TOC Analyzer. DOC was defined as the 0.7 µm Whatman GF/F filtrate of the sample. TOC and DOC measurements in the laboratory gave very low and repeatable analytical blanks (0.029 ± 0.009 ppm, 1 SD), while the operational blanks ranged from 0.088 to 0.099 ppm and are given in Table S3 (Supplementary Information). For comparison, the blank-corrected concentration values and their variability are provided in Table S4 (Supplementary Information). POC concentration (C_{POC}) was obtained from equation 3:

(3) $C_{POC} = C_{TOC} - C_{DOC,}$

where C_{TOC} and C_{DOC} are concentrations of the total and dissolved fractions of OC.

In the case of the cryoconite samples, a chemical digestion method was employed after detecting significant mass loss due to clay particle destruction whilst using the Loss On Ignition method. The organic matter content of the cryoconite samples was therefore established gravimetrically following chemical digestion with 1M KOH. From the mass loss, the OC content was estimated using an OC to organic matter mass ratio of 0.254, which was found in cryoconite on Longyearbreen, a glacier located within 20 km radius from Foxfonna (Hodson et al., 2010b).

Flux calculations

Winter deposition (A^{acc}) was estimated from the arithmetic mean loading of the individual snow cores (Equation 4):

$$(4) \quad A^{acc} = \overline{(SWE \times k_S \times OC^{snow})} \times A_c,$$

where SWE = snow water equivalent, OC^{snow} = concentration of TOC or DOC in the snow cores, k_S = correction applied to account for the corer being too short to sample the entire depth of the snowpack, and A_c = catchment area.

Summer deposition (A^{abl}) was also calculated as an arithmetic mean using Equation 5:

$$(5) \quad A^{abl} = \frac{1}{d_A} \sum_n \overline{V \times OC^{DT} \times a \times k_{DT}} \times A_c,$$

where d_A = fraction of total ablation period monitored using dust traps , n = number of sampling intervals (7-10 days), for which A^{abl} was estimated, and V and OC^{DT} are the volume of water and OC concentration measurements collected at each dust trap. The terms a and k_{DT} represent the trap area (0.0397 m^2) and an efficiency factor as described by Sow et al. (2006).

The calculation of fluvial export (Qc) was achieved using Equation 6:

$$(6) \quad Q_C = 1/d_Q \times Q_{obs} \times \overline{OC},$$

where d_Q = fraction of the runoff season monitored for discharge, Q_{obs} = total observed water flux and $\overline{OC}$ = arithmetic mean of DOC or TOC concentration. The arithmetic mean was suitable for the total flux calculation because of the lack of

dependence of $\overline{OC}$ upon Q_{obs}. The OC concentration values were deduced from the streams at the glacier snout (B2, B3 and B4 sites).

The release of OC from glacier ice (Ic) was calculated using Equation 7:

(7) $\quad Ic = \sum_i (Bn_i \times \overline{OC}^{GI}_i \times A_{z_i})$,

where $\overline{OC}^{GI}_i$ = mean OC content of the melted depth of glacier ice, Bn_i = total depth of melt, A_{z_i} = surface area of each elevation zone. This equation assumes that firn, the previous year's superimposed ice and glacier ice have the same OC concentration, which is unlikely. However, the very small accumulation area of the glacier (see section *Glacial ice melt (Ic)* of *Results*) means contributions from both firn and "old" superimposed ice were negligible in this study.

The transient OC store in superimposed ice (SI) was not included in the annual budget calculations, but was in any case estimated from equation 8:

(8) $SI = \overline{OC}^{SI} \times d_{SI} \times 0.85 \times A_c$,

where $\overline{OC}^{SI}$ = arithmetic mean OC concentration in each superimposed ice core, d_{SI} = superimposed ice thickness, and 0.85 = assumed density in g cm^{-3}.

Estimates of Δbio assumed that NEP was constant in time and equal to the average of measured daily values ($\overline{NEP_d}$). The spatial coverage of cryoconite activity was calculated using Equation 9 (after Cook et al., 2012; Hodson et al., 2010a):

(9) $\quad \Delta bio = \overline{NEP_d} \times \sum_{i=1}^{n}(d \times a \times c \times M_d)$,

where d = number of days when a particular fraction of the glacier surface was free from snow; c = mean proportion of area a that is covered by cryoconite, and M_d =

conversion factor from cryoconite area to dry mass, derived from the complete sampling of ten cryoconite holes of known surface area (0.059 g cm^{-2}) (Cook et al., 2010). The term *d* was estimated from oblique photos of the glacier surface taken every 1–4 days (*n* being the number of those periods), while c was deduced from the 2011 photographic survey across the glacier, mentioned in section *Storage in supraglacial debris (SOC)* of *Materials and methods.*

The above terms were then combined according to equation 10 to provide the total carbon mass balance for the glacier (see Hodson et al. (2005) and Fig 1):

(10)   *A + Ic - Qc ± Δbio = ΔSOC,*

where *ΔSOC* is the change in OC storage on the glacier surface at the end of the ablation season. Since we have accounted for snow and ice, it is most likely to represent a dust layer contributing to cryoconite.

The error estimations for these fluxes are described in *Supplementary Information* and the values are reported together with the results.

Results

Atmospheric deposition (*A*)

Figure 4 and Table 2 show how the deposition of OC varied in space and time. A^{acc} TOC in 2011 (0.138 ± 0.051 Mg a^{-1}) was much smaller than in 2012 (0.484 ± 0.219 Mg a^{-1}), whilst the opposite was the case for A^{abl} TOC (0.473 ± 0.171 Mg a^{-1} in 2011 and 0.172 ± 0.048 Mg a^{-1} in 2012). In the winter of 2012, the distribution of DOC in A^{acc} was uneven, with the middle part of the glacier (500–550 m elevation band) showing the lowest DOC flux. Conversely, in the winter of 2011 the upper

elevation bands contained less DOC than the lower part of the glacier (Fig. 4). Otherwise, TOC concentration variability was closely connected to SWE changes (Spearman rank correlation r = 0.482, p<0.018), unlike DOC concentrations (no significant correlation).

Organic carbon transport by meltwater runoff (Qc)

The runoff at the glacier snout in 2011 was generally more stable than in 2012 (Fig. 5), although two slowdowns in runoff progression occurred in August: due to a snowfall event from 10–12 August 2011, and a cooling towards the end of the ablation season, after 27 August 2011. The second half of August 2012 was characterised by a similarly small amount of runoff. The high flows during each year were linked to snow or ice melt in July, sometimes combined with heavy rainfall (between 7 and 14 July 2011 and around 8 August 2012). The importance of melt was emphasised by a significant correlation between discharge and temperature across both years (Spearman rank r = 0.475, p<0.001).

The OC concentrations in runoff (Fig. 5) showed no significant correlation with discharge nor time of the day (for Q, r = -0.219, p>0.05 for DOC and r = 0.272, p>0.05 for TOC; for diurnal cycle, r = -0.192, p>0.05 for DOC and r = -0.108, p>0.05 for TOC; all data merged for 2011 and 2012). There was, however, a progressive increase in both TOC and DOC concentrations with day number across the melt season, especially in 2012 (r = 0.565, p<0.001 for DOC and r = 0.389, p<0.02 for TOC, in pooled data from both seasons). In the Qc fluxes (Table 2), DOC represented the largest fraction of the TOC runoff yield in both years (67.2 ± 6.6 and 89.5 ± 7.7% in 2011 and 2012, respectively).

Glacial ice melt (*Ic*)

During 2011 and 2012, the net glacier ice mass balance (*Bn*) in the studied catchment was estimated at -0.89 and -0.42 m a^{-1}, respectively. Therefore, glacier ice ablation dominated *Ic* for both TOC and DOC (Table 2 and Figure 7) and is likely to do so every year under the present climatic regime. No superimposed ice accumulation was observed at the end of either summer, although there is likely to have been some within the small firn-covered area (<0.3 km^2) where crevasses and steep slopes prevented its investigation. However, its limited extent and the steep topography that facilitated water runoff both mean that the quantity of OC stored there was trivial. Therefore, the estimated *Ic* fluxes were solely based on *Bn* and the glacial ice OC concentrations, and the 26% difference between the annual TOC fluxes for 2011 and 2012 stemmed mainly from the net mass balance variability. The difference was, however, smaller than the *Bn* difference of 53% due to a high OC concentration in the upper 20 cm layer, which contributed (in 2012) 55% of TOC and 49% of DOC content in the annual *Ic* flux.

Transient store of OC in the superimposed ice (*SI*)

Maximum superimposed ice layer thicknesses during July 2011 and 2012 were 21 (± 2, 1SD) cm and 18 (± 2, 1SD) cm, respectively, indicating a broadly similar quantity of snowmelt refreezing on the glacier surface during the early ablation seasons. This refrozen ice layer was found to represent a flux capturing 0.115 ± 0.042 Mg a^{-1} TOC and 0.081 ± 0.032 Mg a^{-1} DOC in 2011, and 0.129 ± 0.048 Mg a^{-1} TOC and 0.114 ± 0.045 Mg a^{-1} DOC in 2012, when at maximum thickness. The values for 2011, therefore, show that the temporary storage of OC in SI can be the same order of magnitude as the A^{acc} (Table 2). Furthermore, the storage in *SI* was also spatially variable (Figure 4), although less so than snow inputs to the system.

Biological activity (*Δbio*)

Table 3 shows that the *NEP* was on average 10.96 (± 5.31 1SD) µg C g^{-1} day^{-1} in 2011 and 23.43 (± 7.17 1SD) µg C g^{-1} day^{-1} in 2012, implying that the ecosystem was therefore net autotrophic. This is in agreement with the results of incubations conducted in 2009 (Hodson, Unpub. Data; locations A2 and A4). Both *R* and *PP* increased with elevation in 2011 and 2012 (data not shown). The final budget contribution of *Δbio* was, however, small: 0.030 ± 0.095 Mg a^{-1} TOC in 2011 and 0.023 ± 0.071 Mg a^{-1} TOC in 2012.

Long-term storage on the glacier surface (SOC)

The average cryoconite coverage on the glacier was estimated from the image analysis to be 8.25% (± 2.25%, 1 SD), with a debris mass of 56.4 ± 14.0 Mg according to the mass conversion of 0.059 g cm^{-2} and the ablation area. Given the average OC concentration in the debris of 2.03% (±1.20%, 1 SD), the corresponding TOC store in the supraglacial debris was 1.14 ± 0.23 Mg in the end of summer 2011. The lower part of the glacier had both the greatest proportion of its surface covered with cryoconite and the highest OC mass per unit area gathered in this debris layer (Fig. 6).

Discussion

In this study, the OC deposition, storage and export have been measured in a glacial system over two consecutive years. The combined OC budget calculations produced positive estimates for *ΔSOC* during both years (Figure 7). Total atmospheric deposition therefore marginally exceeded the fluvial export, and the biological component was small compared to the other fluxes in both years. As a result, *ΔSOC* was quantitatively similar to *Ic* in both years.

Atmospheric inputs

The atmospheric DOC can originate from human activity (local and distant pollutant emissions; see Kozak et al., 2013; Stubbins et al., 2012), vegetation (e.g. plant emissions of volatile organic compounds, or VOCs; Lindwall et al., 2015), and from excretions of the airborne organisms, such as bacteria (Sattler et al., 2001). Due to the sampling of winter deposition in the end of the season, it may also include DOC that comes from post-depositional transformations of POC, e.g. through photodegradation or supraglacial ecosystem activity in decomposing e.g. humic-like compounds. Furthermore, the dry deposition of gaseous organic compounds may also contribute to the final DOC content of snow (see also McNeill et al., 2012). Among POC, bigger microbial cells should be counted (the threshold 0.7 μm particle diameter being higher than cell size of some microbes), alongside wind-blown plant tissue, organic-rich rock and soil dusts, particles related to human activity, and secondary aerosols formed through aggregation of airborne particles.

OC concentrations in the snow were highly variable and subject to the highest error brackets among the OC fluxes, but the means were consistent with other studies (e.g. Xu et al., 2006; Yan et al., 2015). Lafrenière and Sharp (2011) found higher DOC concentrations (280 – 410 ppb) in mature low-latitude snow perhaps indicating the OC content of lower latitude snow might be greater than in the High Arctic due to more abundant vegetation in and around the catchment. The connection between proximity to vegetation and OC content of snow is also consistent with the pattern of mostly allochthonous OC on small glaciers (Stibal et al., 2008) and the observations of macroscopic plant fragments on the surface of Foxfonna. It is likely that windborne transport is also important, given the intensive wind redeposition of snow observed in this site and the interdependence of TOC

concentration and SWE. However, this latter relationship may be partly invoked by the scavenging of OC during snowfall (Kang et al., 2009).

The OC flux from winter snow deposition may be reduced by post-depositional processes, including photo-oxidation during the spring and summer season (Grannas et al., 2004). Photodegradational loss of organic matter from Arctic snowpack of 0.480-4.08 mg C m^{-2} d^{-1} was estimated by Voisin et al. (2012), indicating a potentially important but poorly constrained component of the glacial carbon budget. Furthermore, this process is a potential mechanism of transformation of POC into DOC. Its impact was limited in this study by the late sampling and the consideration of net A^{acc} value.

Rates of atmospheric OC deposition at Foxfonna were highly variable in both space and time. Temporal variation between the two years of monitoring (Table 2 and Figure 7) can be explained by meteorological conditions during the sampling periods. In July 2011, 16 mm of rainfall fell over the catchment in one week, enhancing A^{abl} (Fig. 3). Other unusual meteorological events included winter rainfall and late-spring snowfall in 2012. High precipitation events are usually associated with warm air inflow to Svalbard from southerly latitudes, which may deliver industrial pollutants (e.g. Hodson et al., 2009; Krawczyk et al., 2008; Kühnel et al., 2013). To better predict glacial carbon budgets, a framework for determining the impact of individual meteorological events is required.

Fluvial export

Fluvial export of TOC and DOC from the glacier surface were similar between years (Table 2). The Qc flux for DOC (0.27 g m^{-2} yr^{-1} in both years) was also consistent with Singer et al's (2012) estimate of 0.17 g C m^{-2} yr^{-1} for glaciers in the European Alps. DOC concentrations in runoff reported here are also similar to those

found in other studies (Bhatia et al., 2013; Downes et al., 1986; Hood et al., 2009; Lafrenière and Sharp, 2011) which showed mean annual concentrations of 0.1−4.1 ppm. Our data from Foxfonna (0.35 ppm in 2011 and 0.25 ppm in 2012) are at the lower end of this range, perhaps due to smaller contributions from subglacial and forefield processes compared to other sites (Bhatia et al., 2013; Downes et al., 1986; Hood et al., 2009).

The seasonal increase in TOC and DOC of Foxfonna proglacial runoff may be connected to a shift in hydrological regime. A clear change in runoff amplitudes after 28th July 2012 coincided with the supraglacial catchment losing most of its snow cover, exposing supraglacial stores of OC. Future studies should test this hypothesis because this will impact estimates of OC release from glaciers with consequences for downstream extraglacial ecosystems (Bradley et al., 2016; Fellman et al., 2015; Hood et al., 2015).

Liberation of OC from melting glacier ice and supraglacial biological activity

Mean OC concentrations in Foxfonna glacial ice were 0.933 ppm in the upper 20 cm and 0.410 ppm for the rest of the 1 m core, due to a strong negative down-core gradient. This is higher than reported by Jenk et al. (2009) in a deep Alpine ice core (0.015 – 0.066 ppm). This suggests that the near surface ice might represent a store of OC. Since Foxfonna is a predominantly cold polythermal glacier, the melting isotherm is often very close to the surface. A thin surface layer of ice acts as a shallow perched aquifer through which OC can be transported in flowing meltwater. This is often referred to as the *weathering crust* (Cook et al., 2016; Irvine-Fynn et al., 2011). It is also the most likely environment for the transformation of DOC into POC and the opposite; through dissolution, adsorption, microbial decomposition of organic matter or growth, and photodegradation.

Biological activity in the surface layer of ice may explain some of the additional OC found there, either because OC is leached from cryoconite (Cook et al., 2016) or the weathering crust is a distinct habitat in its own right (Edwards et al., 2014), sometimes referred to as "dirty ice" (Musilova et al., 2017). On Foxfonna, the upper 20 cm of glacial ice is a small store of OC compared to the cryoconite. Even if all the carbon stored in the uppermost glacial ice was produced in situ, the flux related to biological production there would still be an order of magnitude smaller than the glacier-wide supraglacial carbon storage in cryoconite.

The magnitudes of surface OC storage suggest that probably the most important biological OC flux is related to cryoconite. Its *NEP* values on Foxfonna are high compared to those from other glaciers in the area, where a net heterotrophic system (*R*>*PP*) has been reported (Stibal et al., 2008; Telling et al., 2010). Stibal et al. (2008) measured *PP* on Werenskiöld glacier, Svalbard, to be *c.* 4.3 µg C g^{-1} yr^{-1}, whilst Telling et al. (2010) reported *PP* rates of 17.3 µg C g^{-1} d^{-1}, a mean *R* of 20.1 µg C g^{-1} d^{-1} and *NEP* of -1.3 µg C g^{-1} d^{-1} for three Svalbard glaciers located near Ny Ålesund. Although it is unclear whether cryoconite ecosystems are mostly net autotrophic or net heterotrophic, the finding from this study that the *Δbio* connected to cryoconite is a very small component of the entire OC budget is important. Furthermore, since the *NEP* values found on Foxfonna are an order of magnitude higher than on other Svalbard glaciers, it is likely that the flux is also negligible in other, similar settings.

A second active microbial habitat is surface algal blooms found on snow or ice. In Greenland these were found to promote net autotrophy both on the GrIS and the Mittivakat glacier (Lutz et al., 2014; Yallop et al., 2012), contributing to ice surface darkening. However, intense blooms were not observed on Foxfonna and they are

not widespread on Svalbard glaciers. Occasional snow algal blooms, with moderate biomass, do result in red colouration of the snow surface where snow is melting. Therefore, this issue will be treated here as an unquantified error in ΔSOC. Any significant biological activity in the snow would even increase the estimated net retention of OC upon Foxfonna calculated here.

The relation between OC fluxes and its long-term storage

Accumulation and ablation conditions varied between 2011 and 2012, yet ΔSOC was similar. This suggests net retention of OC is typical for this glacier. Cryoconite debris is probably the dominant OC store. This is supported by estimating the quantity of ΔSOC that was particulate (i.e. "ΔSOC^{POC}") and the magnitude of OC in cryoconite deposits (Equation 11):

(11) $\Delta SOC^{POC} = \Delta SOC^{TOC} - \Delta SOC^{DOC}$,

ΔSOC^{POC} was 0.310 ± 0.109 Mg a^{-1} in 2011 and 0.424 ± 0.117 Mg a^{-1} in 2012. In this case, ΔSOC^{POC} accumulation over $c.$ 3 years would account for the cryoconite SOC store (1.14 ± 0.23 Mg). Since cryoconite holes are known to persist over timescales of years to decades (Hodson et al., 2010b; Takeuchi et al., 2010) cryoconite is a plausible sink for the excess ΔSOC^{POC} in this study.

Supraglacial processes that disturb and redistribute cryoconite will regulate the residence time of supraglacial OC to some extent. In particular, wash-out or melt-out of cryoconite holes during periods of turbulent heat flux dominated energy balance, rainfall or extreme surface melt and invasion of cryoconite holes by supraglacial rills, streams and crevasses are potential redistribution mechanisms (Cook et al., 2016).

An important part of the glacial OC fluxes is the dissolved organic matter, which comprises 63% of the combined atmospheric flux, 53% of the release from ice melt,

77% of riverine OC and 80% of the transient superimposed ice store. By contrast, it represented between just 54% (2011) and 36% (2012) of *ΔSOC,* DOC is therefore more likely to be transferred to the glacier forefield by runoff than POC, and thus influence downstream ecosystems (Hood et al., 2009).

Conclusions

This study provides a simultaneous investigation of inputs, throughputs and outputs of organic carbon (OC) upon an Arctic glacier surface. Comparison of the fluxes shows net retention of OC is likely a common occurrence. The physical retention concerns both the allochthonous inputs of atmospheric OC and the OC released from the uppermost layers of glacier ice by surface melt. The estimated rates of storage of particulate OC (POC) were consistent across the two years (2011 and 2012) and represented enough OC to supply the amount of carbon associated with cryoconite debris within *c.* 3 years. This surface carbon may contribute to glacier surface darkening, raising the pressing need to better understand the long-term fate of supraglacial OC storage, and its feedback to melt processes, including the physical redistribution this OC is undergoing.

The processes leading to apparent OC accumulation on the glacier surface need to be balanced by a yet unknown process in the long-term, or else the supraglacial layer of POC would be increasing indefinitely and eventually suppress ablation. Therefore, two potentially important processes involved in the removal of POC from the glacier surface are proposed here: organic-rich debris erosion during extreme melt or rainfall events, and POC transfer to internal storage within the glacier. The former process would drive irregular supplies of OC to the glacier forefield and could supply nutrient to downstream ecosystems. The latter would increase the lag between OC release from melting ice and its removal from the site, which could lead

to multiple cycles of the same particle burial and re-emergence on the glacier surface.

The processes leading to OC retention are active also for dissolved organic species, despite these being removed more rapidly from the glacier surface than POC. The highest ratio of dissolved to total organic carbon was found in the refrozen meltwaters (superimposed ice) and supraglacial runoff, and hence the superimposed ice is proposed here as an important temporary store for dissolved OC. Yet, it is unclear how this medium obtains and releases its OC content, for which we recommend further investigation, as we do for the underexplored way of OC transformation which is photodegradation.

References

Anesio AM, Hodson AJ, Fritz A, Psenner R, Sattler B. 2009. High microbial activity on glaciers: importance to the global carbon cycle. *Global Change Biology* 15 : 955–960. DOI: 10.1111/j.1365-2486.2008.01758.x

Bhatia MP, Das SB, Xu L, Charette MA, Wadham JL, Kujawinski EB. 2013. Organic carbon export from the Greenland ice sheet. *Geochimica et Cosmochimica Acta* 109 : 329–344. DOI: 10.1016/j.gca.2013.02.006

Bøggild CE, Brandt RE, Brown KJ, Warren SG. 2010. The ablation zone in northeast Greenland: ice types, albedos and impurities. *Journal of Glaciology* 56 : 101–113. DOI: 10.3189/002214310791190776

Bradley JA et al. 2016. Microbial dynamics in a High Arctic glacier forefield: a combined field , laboratory , and modelling approach. *Biogeosciences* 13 : 5677–5696. DOI: 10.5194/bg-13-5677-2016

Chandler DM, Alcock JD, Wadham JL, MacKie SL, Telling J. 2015. Seasonal changes of ice surface characteristics and productivity in the ablation zone of the Greenland Ice Sheet. *Cryosphere* : 487–504. DOI: 10.5194/tc-9-487-2015

Cook J, Hodson A, Telling J, Anesio A, Irvine-Fynn TD, Bellas C. 2010. The mass–area relationship within cryoconite holes and its implications for primary production. *Annals of Glaciology* 51 : 106–110. DOI: 10.3189/172756411795932038

Cook JM, Hodson AJ, Anesio AM, Hanna E, Yallop M, Stibal M, Telling J, Huybrechts P. 2012. An improved estimate of microbially mediated carbon fluxes from the Greenland ice sheet. *Journal of Glaciology* 58 : 1398–1408. DOI: 10.3189/2012JoG12J001

Cook JM, Hodson AJ, Gardner AS, Flanner M, Tedstone AJ, Williamson C, Irvine-

Fynn TD, Nilsson J, Bryant R, Tranter M. 2017. Quantifying bioalbedo: A new physically-based model and critique of empirical methods for characterizing biological influence on ice and snow albedo. *The Cryosphere Discussions* : 1–29. DOI: 10.5194/tc-2017-73

Cook JM, Hodson AJ, Irvine-Fynn TDL. 2016. Supraglacial weathering crust dynamics inferred from cryoconite hole hydrology. *Hydrological Processes* 30 : 433–446. DOI: 10.1002/hyp.10602

Downes MT, Howard-Williams C, Vincent WF. 1986. Sources of organic nitrogen, phosphorus and carbon in Antarctic streams. *Hydrobiologia* 134 : 215–225.

Edwards A, Irvine-Fynn T, Mitchell AC, Rassner SME. 2014. A germ theory for glacial systems? *WIREs Water* 1 : 331–340. DOI: 10.1002/wat2.1029

Fellman JB, Hood E, Raymond PA, Hudson J, Bozeman M, Arimitsu M. 2015. Evidence for the assimilation of ancient glacier organic carbon in a proglacial stream food web. *Limnology and Oceanography* 60 : 1118–1128. DOI: 10.1002/lno.10088

Gardner AS, Moholdt G, Wouters B, Wolken GJ, Burgess DO, Sharp MJ, Cogley JG, Braun C, Labine C. 2011. Sharply increased mass loss from glaciers and ice caps in the Canadian Arctic Archipelago. *Nature* 473 : 357–60. DOI: 10.1038/nature10089

Grannas AM, Shepson PB, Filley TR. 2004. Photochemistry and nature of organic matter in Arctic and Antarctic snow. *Global Biogeochemical Cycles* 18 DOI: 10.1029/2003GB002133

Hodgkins R. 2001. Seasonal evolution of meltwater generation, storage and discharge at a non-temperate glacier in Svalbard. *Hydrological Processes* 15 : 441–460.

Hodson A, Roberts TJ, Engvall A-C, Holmén K, Mumford P. 2009. Glacier ecosystem response to episodic nitrogen enrichment in Svalbard, European High Arctic. *Biogeochemistry* 98 : 171–184. DOI: 10.1007/s10533-009-9384-y

Hodson AAJ, Anesio AM, Tranter M, Fountain A, Osborn M, Priscu JC, Laybourn-Parry J, Sattler B. 2008. Glacial ecosystems. *Ecological Monographs* 78 : 41–67. DOI: 10.1890/07-0187.1

Hodson AJ et al. 2007. A glacier respires?: Quantifying the distribution and respiration CO2 flux of cryoconite across an entire Arctic supraglacial ecosystem. 112 : 1–9. DOI: 10.1029/2007JG000452

Hodson AJ, Bøggild C, Hanna E, Huybrechts P, Langford H, Cameron K, Houldsworth A. 2010a. The cryoconite ecosystem on the Greenland ice sheet. *Annals of Glaciology* 51 : 123–129. DOI: 10.3189/172756411795931985

Hodson AJ, Cameron K, Bøggild C, Irvine-Fynn T, Langford H, Pearce D, Banwart S. 2010b. The structure, biological activity and biogeochemistry of cryoconite aggregates upon an Arctic valley glacier: Longyearbreen, Svalbard. *Journal of Glaciology* 56 : 349–362. DOI: 10.3189/002214310791968403

Hodson AJ, Mumford PN, Kohler J, Wynn PM. 2005. The High Arctic glacial ecosystem: new insights from nutrient budgets. *Biogeochemistry* 72 : 233–256. DOI: 10.1007/s10533-004-0362-0

Hood E, Battin TJ, Fellman J, O'Neel S, Spencer RGM. 2015. Storage and release of organic carbon from glaciers and ice sheets. *Nature Geoscience* : 1–6. DOI: 10.1038/ngeo2331

Hood E, Berner L. 2009. Effects of changing glacial coverage on the physical and biogeochemical properties of coastal streams in southeastern Alaska. *Journal of*

Geophysical Research 114 : G03001. DOI: 10.1029/2009JG000971

Hood E, Fellman J, Spencer RGM, Hernes PJ, Edwards R, D'Amore D, Scott D. 2009. Glaciers as a source of ancient and labile organic matter to the marine environment. *Nature* 462 : 1044–1048. DOI: 10.1038/nature08580

Irvine-Fynn TD., Bridge JW, Hodson AJ. 2010. Rapid quantification of cryoconite: granule geometry and in situ supraglacial extents, using examples from Svalbard and Greenland. *Journal of Glaciology* 56 : 297–308. DOI: 10.3189/002214310791968421

Irvine-Fynn TDL, Hodson AJ, Moorman BJ, Vatne G, Hubbard AL. 2011. Polythermal glacier hydrology: a review. *Reviews of Geophysics* 49 : 1–37. DOI: 10.1029/2010RG000350

Jenk TM, Szidat S, Bolius D, Sigl M, Gäggeler HW, Wacker L, Ruff M, Barbante C, Boutron CF, Schwikowski M. 2009. A novel radiocarbon dating technique applied to an ice core from the Alps indicating late Pleistocene ages. *Journal of Geophysical Research* 114 : D14305. DOI: 10.1029/2009JD011860

Kang J-H, Choi S-D, Park H, Baek S-Y, Hong S, Chang Y-S. 2009. Atmospheric deposition of persistent organic pollutants to the East Rongbuk Glacier in the Himalayas. *The Science of the Total Environment* 408 : 57–63. DOI: 10.1016/j.scitotenv.2009.09.015

Kozak K, Polkowska Ż, Ruman M, Kozioł K, Namieśnik J. 2013. Analytical studies on the environmental state of the Svalbard Archipelago provide a critical source of information about anthropogenic global impact. *TrAC - Trends in Analytical Chemistry* 50 : 107–126. DOI: 10.1016/j.trac.2013.04.016

Koziol K. 2014. The provenance, composition and fate of organic carbon on an

Arctic glacier. PhD thesis, University of Sheffield & University Centre in Svalbard (UNIS)

Krawczyk WE, Bartoszewski SA, Siwek K. 2008. Rain water chemistry at Calypsobyen, Svalbard. *Polish Polar Research* 29 : 149–162.

Kühnel R, Björkman MP, Vega CP, Hodson AJ, Isaksson E, Ström J. 2013. Reactive nitrogen and sulphate wet deposition at Zeppelin Station, Ny-Ålesund, Svalbard. *Polar Research* 32 : 19136. DOI: http://dx.doi.org/10.3402/polar.v32i0.19136

Lafrenière MJ, Sharp MJ. 2011. The Concentration and Fluorescence of Dissolved Organic Carbon (DOC) in Glacial and Nonglacial Catchments: Interpreting Hydrological Flow Routing and DOC Sources. *Arctic, Antarctic and Alpine Research* 36 : 156–165.

Lawson EC, Wadham JL, Tranter M, Stibal M, Lis GP, Butler CEH, Laybourn-Parry J, Nienow P, Chandler D, Dewsbury P. 2014. Greenland Ice Sheet exports labile organic carbon to the Arctic oceans. *Biogeosciences* 11 : 4015–4028. DOI: 10.5194/bg-11-4015-2014

Liestøl O. 1974. Glaciological work in 1972. In Årbok 1972 , . Norsk Polarinstitutt: Oslo; 125–135.

Lindwall F, Faubert P, Rinnan R. 2015. Diel variation of biogenic volatile organic compound emissions- A field study in the sub, low and high arctic on the effect of temperature and light. *PLoS ONE* 10 : 1–24. DOI: 10.1371/journal.pone.0123610

Liu Y, Xu J, Kang S, Li X, Li Y. 2016. Storage of dissolved organic carbon in Chinese glaciers. *Journal of Glaciology* 62 : 402–406. DOI: 10.1017/jog.2016.47

Lutz S, Anesio AM, Jorge Villar SE, Benning LG. 2014. Variations of algal

communities cause darkening of a Greenland glacier. *FEMS Microbiology Ecology* 89 : 402–14. DOI: 10.1111/1574-6941.12351

McNeill VF et al. 2012. Organics in environmental ices: sources, chemistry, and impacts. *Atmospheric Chemistry and Physics Discussions* 12 : 8857–8920. DOI: 10.5194/acpd-12-8857-2012

Moholdt G, Nuth C, Hagen JO, Kohler J. 2010. Recent elevation changes of Svalbard glaciers derived from ICESat laser altimetry. *Remote Sensing of Environment* 114 : 2756–2767. DOI: 10.1016/j.rse.2010.06.008

Musilova M, Tranter M, Wadham J, Telling J, Tedstone A, Anesio AM. 2017. Microbially driven export of labile organic carbon from the Greenland ice sheet. *Nature Geoscience* 10 : 360–365. DOI: 10.1038/ngeo2920

Priscu JC, Tulaczyk S, Studinger M, Kennicutt MC, Christner BC, Foreman CM. 2008. Antarctic Subglacial Water: origin, evolution and ecology. In Polar Lakes and Rivers: Limnology of Arctic and Antarctic Aquatic Ecosystems , Laybourn-Parry J and Vincent WF (eds). Oxford University Press; 119–135.

Sattler B, Puxbaum H, Psenner R. 2001. Bacterial growth in supercooled cloud droplets. *Geophysical Research Letters* 28 : 239–242.

Schlesinger WH, Bernhardt ES. 2013. Biogeochemistry: an analysis of global change . 3rd ed. Academic Press, Elsevier: Oxford

Singer GA, Fasching C, Wilhelm L, Niggemann J, Steier P, Dittmar T, Battin TJ. 2012. Biogeochemically diverse organic matter in Alpine glaciers and its downstream fate. *Nature Geoscience* 5 : 710–714. DOI: 10.1038/ngeo1581

Sow M, Goossens D, Rajot JL. 2006. Calibration of the MDCO dust collector and of four versions of the inverted frisbee dust deposition sampler. *Geomorphology* 82 :

360–375. DOI: 10.1016/j.geomorph.2006.05.013

Stibal M, Lawson EC, Lis GP, Mak KM, Wadham JL, Anesio AM. 2010. Organic matter content and quality in supraglacial debris across the ablation zone of the Greenland ice sheet. *Annals of Glaciology* 51 : 1–8. DOI: 10.3189/172756411795931958

Stibal M, Šabacká M, Žárský J. 2012a. Biological processes on glacier and ice sheet surfaces. *Nature Geoscience* 5 : 771–774. DOI: 10.1038/ngeo1611

Stibal M, Telling J, Cook J, Mak KM, Hodson AJ, Anesio AM. 2012b. Environmental controls on microbial abundance and activity on the greenland ice sheet: a multivariate analysis approach. *Microbial ecology* 63 : 74–84. DOI: 10.1007/s00248-011-9935-3

Stibal M, Tranter M, Benning LG, Řehák J. 2008. Microbial primary production on an Arctic glacier is insignificant in comparison with allochthonous organic carbon input. *Environmental Microbiology* 10 : 2172–8. DOI: 10.1111/j.1462-2920.2008.01620.x

Stubbins A et al. 2012. Anthropogenic aerosols as a source of ancient dissolved organic matter in glaciers. *Nature Geoscience* 5 : 198–201. DOI: 10.1038/ngeo1403

Takeuchi N. 2002. Optical characteristics of cryoconite (surface dust) on glaciers: the relationship between light absorbency and the property of organic matter contained in the cryoconite. *Annals of Glaciology* 34 : 409–414.

Takeuchi N, Kohshima S, Seko K. 2001. Structure, Formation, and Darkening Process of Albedo-Reducing Material (Cryoconite) on a Himalayan Glacier: A Granular Algal Mat Growing on the Glacier. *Arctic, Antarctic, and Alpine Research* 33 : 115–122.

Takeuchi N, Nagatsuka N, Uetake J, Shimada R. 2014. Spatial variations in impurities (cryoconite) on glaciers in northwest Greenland. *Bulletin of Glaciological Research* 32 : 85–94. DOI: 10.5331/bgr.32.85

Takeuchi N, Nishiyama H, Li Z. 2010. Structure and formation process of cryoconite granules on Urűmqi glacier No. 1, Tien Shan, China. *Annals of Glaciology* 51 : 9–14.

Telling J, Anesio AM, Hawkings J, Tranter M, Wadham JL, Hodson AJ, Yallop ML. 2010. Measuring rates of gross photosynthesis and net community production in cryoconite holes: a comparison of field methods. *Annals of Glaciology* 51 : 153–162.

Telling J, Anesio AM, Tranter M, Stibal M, Hawkings J, Irvine-Fynn T, Hodson A, Butler C, Yallop M, Wadham J. 2012. Controls on the autochthonous production and respiration of organic matter in cryoconite holes on high Arctic glaciers. *Journal of Geophysical Research* 117 : G01017. DOI: 10.1029/2011JG001828

Voisin D et al. 2012. Carbonaceous species and humic like substances (HULIS) in Arctic snowpack during OASIS field campaign in Barrow. *Journal of Geophysical Research* 117 : D00R19. DOI: 10.1029/2011JD016612

Xu B, Cao J, Joswiak DR, Liu X, Zhao H, He J. 2012. Post-depositional enrichment of black soot in snow-pack and accelerated melting of Tibetan glaciers. *Environmental Research Letters* 7 : 014022. DOI: 10.1088/1748-9326/7/1/014022

Xu B, Yao T, Liu X, Wang N. 2006. Elemental and organic carbon measurements with a two-step heating–gas chromatography system in snow samples from the Tibetan Plateau. *Annals of Glaciology* 43 : 257–262. DOI: 10.3189/172756406781812122

Xu J, Zhang Q, Li X, Ge X, Xiao C, Ren J, Qin D. 2013. Dissolved organic matter

and inorganic ions in a central Himalayan glacier--insights into chemical composition and atmospheric sources. *Environmental Science & Technology* 47 : 6181–8. DOI: 10.1021/es4009882

Yallop ML et al. 2012. Photophysiology and albedo-changing potential of the ice algal community on the surface of the Greenland ice sheet. *The ISME Journal (Multidisciplinary Journal of Microbial Ecology)* 6 : 2302–13. DOI: 10.1038/ismej.2012.107

Yan F, Kang S, Chen P, Bai J, Li Y, Hu Z, Li C. 2015. Concentration and Source of Dissolved Organic Carbon in Snowpits of the Tibetan Plateau. *Huanjing Kexue* 36 : 2827–2832.

Table 1. Literature review on glacial OC flux estimations to date.

Glacial OC flux type (or concentration which may be used to derive it)	OC type	Value	Location	Reference
Atmospheric deposition				
Concentrations in snowpits	DOC	[µg C L^{-1}] 519.7 ± 136.3 658.7 ± 78.9 642.3 ± 499.1	Glaciers in China: Tien Shan Glacier No. 1 (TS) Laohugou Glacier No. 12 (LHG)	(Liu et al., 2016)
Deposition rates	DOC	~19.8 ± 1.0 Gg a^{-1}	Total rate for all Chinese glaciers	(Liu et al., 2016)
Meltwater and runoff				
Release through melt	DOC	~15.4 ± 6.1 Gg a^{-1}	Total rate for all Chinese glaciers	(Liu et al., 2016)
Proglacial river runoff concentrations and flux	DOC POC	 0.1-4.1 ppm 4.1-13.2 ppm ≈ 0.9 Tg a^{-1}	Greenland Antarctic Southern Alaska Banff National Park, Alberta, Canada Greenland	(Bhatia et al., 2013) (Downes et al., 1986) (Hood and Berner, 2009) (Lafrenière and Sharp, 2011) (Bhatia et al., 2013)
Runoff flux	DOC POC	0.52 – 0.56 Gg a^{-1} ≈ 0.9 g m^{-2} a^{-1} 0.13–0.17 Tg a^{-1} 0.36–1.52 Tg a^{-1}	Leverett Glacier, Greenland Upscaled to Greenland Ice Sheet	(Lawson et al., 2014)
Runoff flux	DOC	0.34 Gg a^{-1} ≈ 0.17 g m^{-2} a^{-1}	European Alps	(Singer et al., 2012)
Glacier runoff	DOC POC	1.04 ± 0.18 TgC yr^{-1} 0.58 ± 0.07 TgC yr^{-1} 1.97 Tg yr^{-1} 0.70 Tg yr^{-1}	Worldwide Mountain glaciers Worldwide Mountain glaciers	(Hood et al., 2015)
Biological fluxes				
Supraglacial ecosystem OC fixing	OC	64 Gg a^{-1}	Global estimate (during the summer season)	(Anesio et al., 2009)
Average glacial	OC	1.3 µg C g^{-1} d^{-1}	a selection of	(Telling et al.,

			Svalbard glaciers	2010)
ecosystem productivity rates				
Photosynthesis and respiration fluxes	OC	10^1–10^2 Gg C a^{-1}	Greenland Ice Sheet	(Hodson et al., 2010a)
Storage				
Supraglacial storage in cryoconite	OC	0.213 g TOC m^{-2} (or 213 kg TOC km^{-2}).	Midtre Lovénbreen, Svalbard	Estimate based on debris mass from Hodson et al. (2007) and OC content of this debris by Telling et al. (2012)
Storage in glacier ice	DOC	~3.96 ± 0.87 Tg	Estimated for all Chinese glaciers	(Liu et al., 2016)
Englacial storage	OC	15.4 Pg	Worldwide	(Priscu et al., 2008)
Storage in glacier ice	DOC	4.48 ± 2.79 Pg 0.07 ± 0.01 Pg	Global (all glaciers and ice sheets) Mountain glaciers	(Hood et al., 2015)

Table 2. Organic carbon (OC) fluxes [Mg a^{-1}] of Foxfonna glacier in 2011 and 2012. Note that *ΔSOC* is a value calculated from Equation 10 for comparison purposes.

Year		2011		2012	
Flux		TOC	DOC	TOC	DOC
Budget components					
A	A^{acc}	0.138 (± 0.051)	0.037 (± 0.050)	0.484 (± 0.219)	0.233 (± 0.196)
	A^{abl}	0.473 (± 0.171)	0.377 (± 0.142)	0.172 (± 0.048)	0.145 (± 0.046)
Qc		0.522 (± 0.040)	0.351 (± 0.027)	0.401 (± 0.032)	0.358 (± 0.029)
Ic		0.513 (± 0.174)	0.259 (± 0.112)	0.382 (± 0.130)	0.216 (± 0.094)
Δbio		0.030 (± 0.095)	-	0.023 (± 0.071)	-
ΔSOC		0.632 (± 0.121)	0.322 (± 0.095)	0.660 (± 0.121)	0.236 (± 0.112)
Temporary storage[a]					
SI		0.099 (± 0.037)	0.070 (± 0.028)	0.114 (± 0.042)	0.101 (± 0.040)

[a] This denotes superimposed ice at the maximum of its formation (late July). This term is not a part of the budget sum since ablation in both years exceeded the refrozen layer thickness.

Table 3. Components of biological growth (Equation 4) in µg C g^{-1} sediment day^{-1} (± 1 SD).

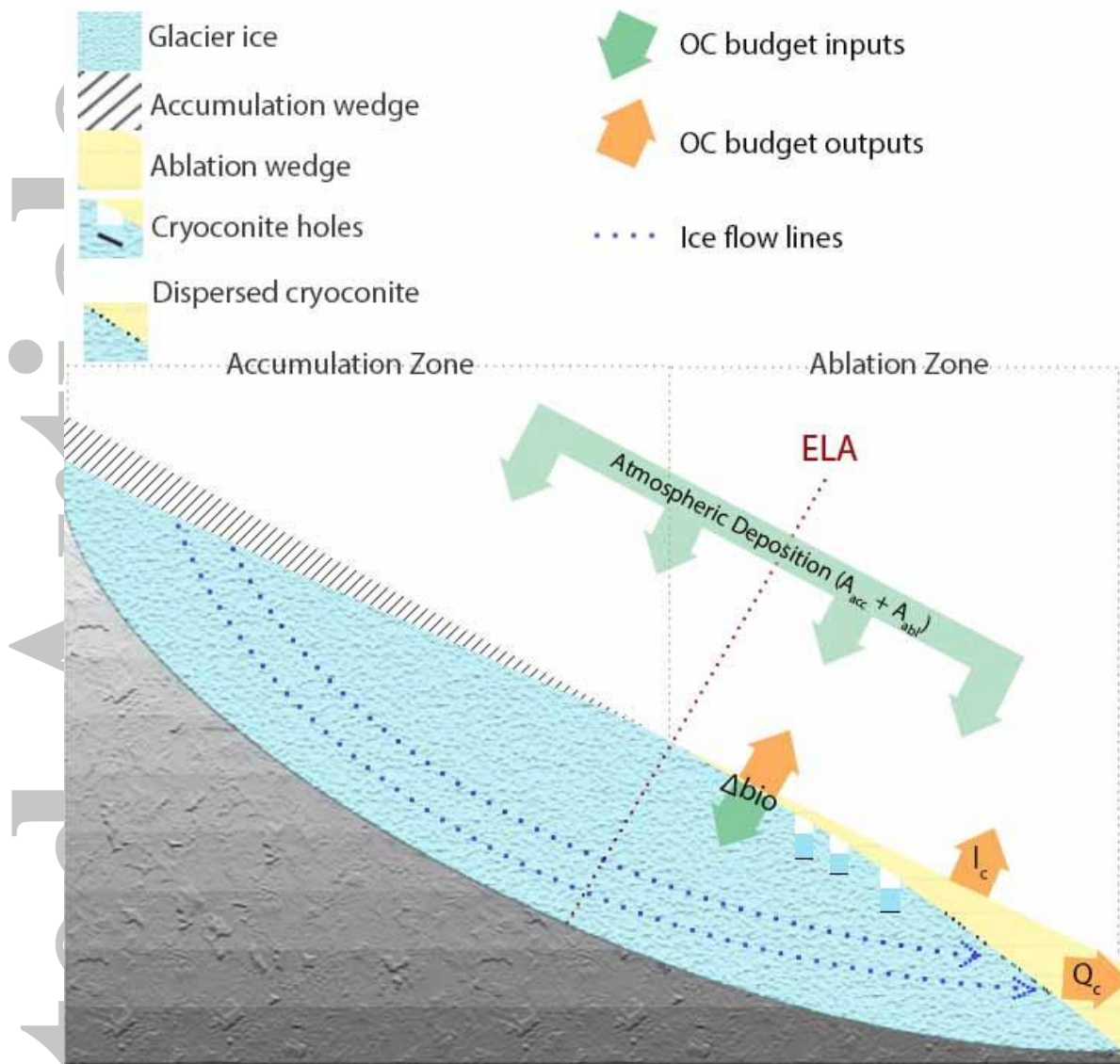| *Δbio* component	2011	2012
NEP	10.96 ± 5.31	23.43 ± 7.17
PP	24.14 ± 4.90	36.30 ± 10.09
R	13.19 ± 1.96	12.87 ± 5.98

Fig. 1. Conceptual understanding of the important OC fluxes on the glacier surface. Abbreviations as in Equations 1-7.
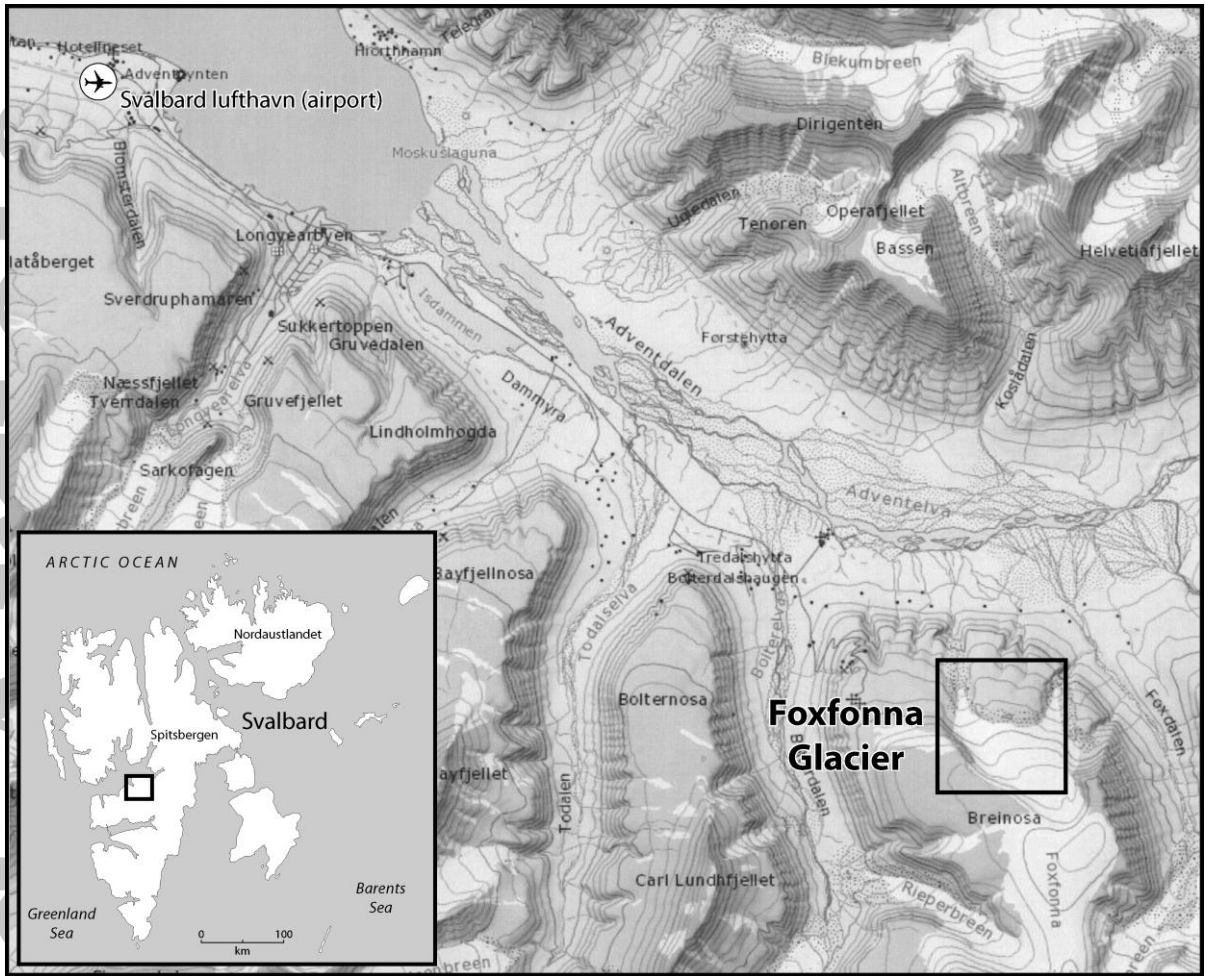
Fig. 2. Location of the study area. Background map source: toposvalbard.npolar.no, courtesy Norwegian Polar Institute.
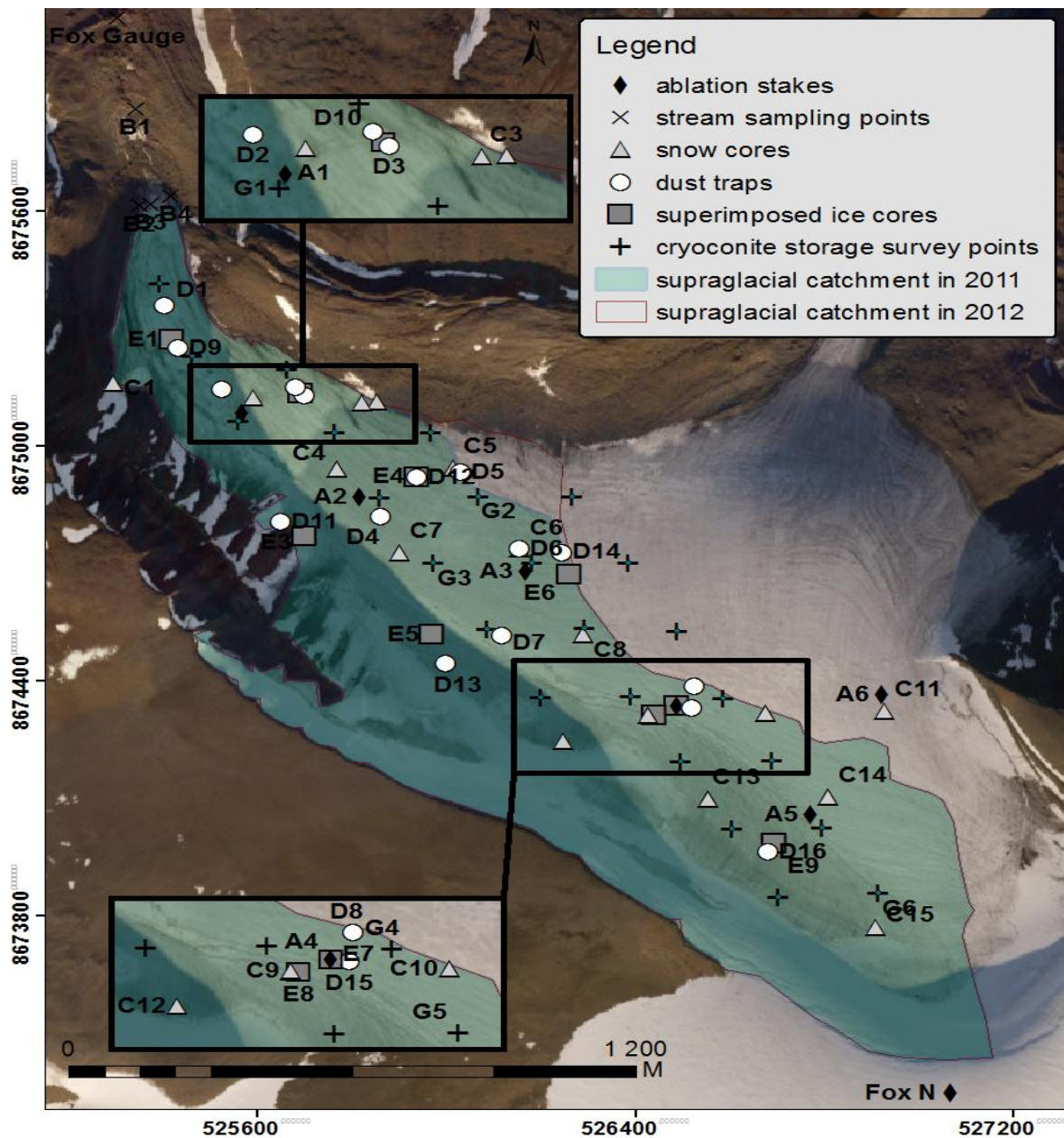
Fig. 3. Sampling points on Foxfonna glacier in 2011 and 2012, showing ablation stakes (A1-6, Fox N), stream sampling locations (B1-4), snow cores (C1-15), dust traps (D1-16), superimposed ice sampling points (E1-9) and glacial ice cores (G1-6). Fox Gauge denotes the location of 2011 discharge monitoring station, and the green catchment area applies to 2011. Background orthophotomap (2006) was made available by Store Norske Spitsbergen Kulkompani AS.
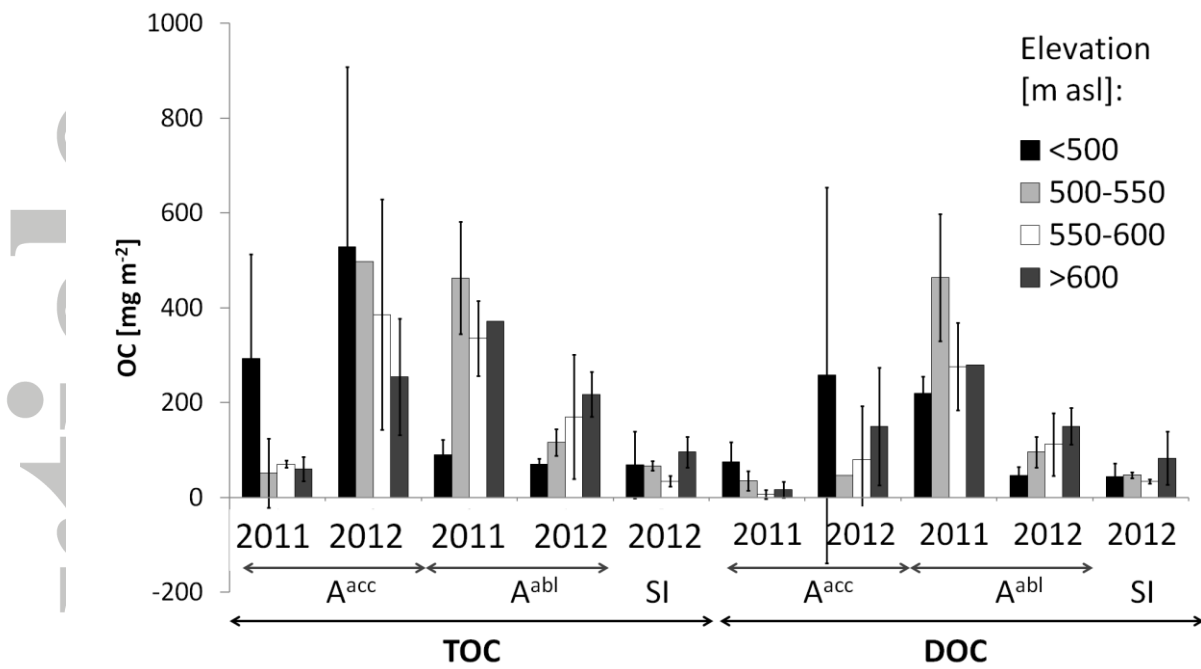
Fig. 4. Variability of atmospheric deposition of OC (per unit area) in the accumulation (A^{acc}) and ablation season (A^{abl}), and the amount of transient storage as superimposed ice (*SI*): all in 50 m elevation zones on Foxfonna glacier. Where more than one value contributed to the mean, 1 SD error bars are shown.
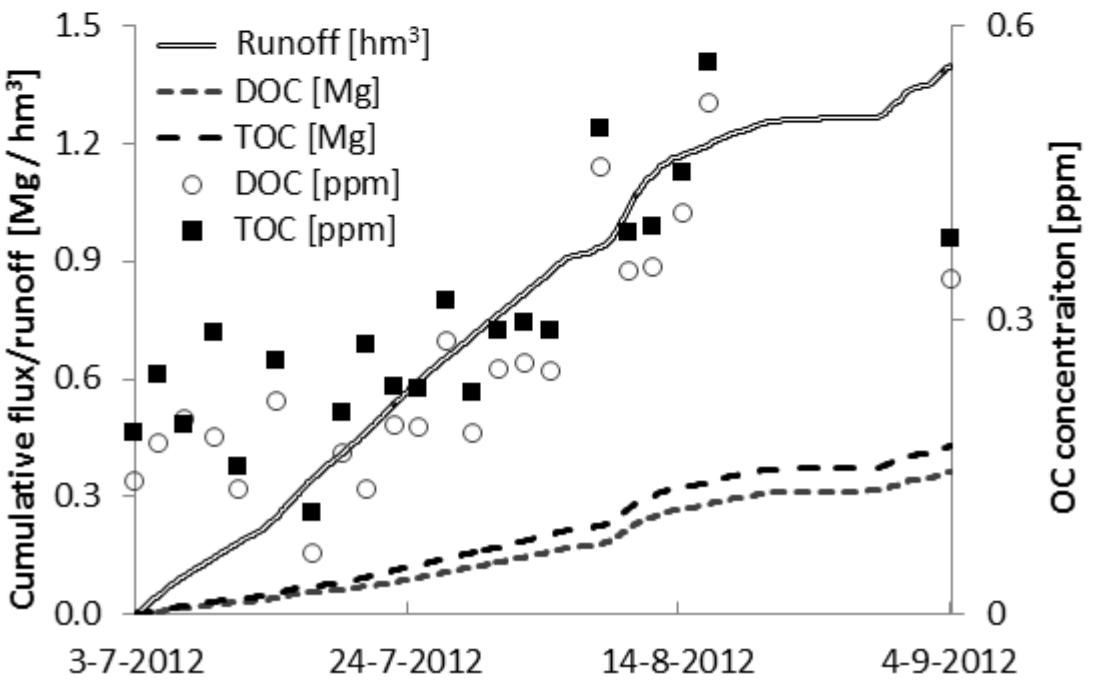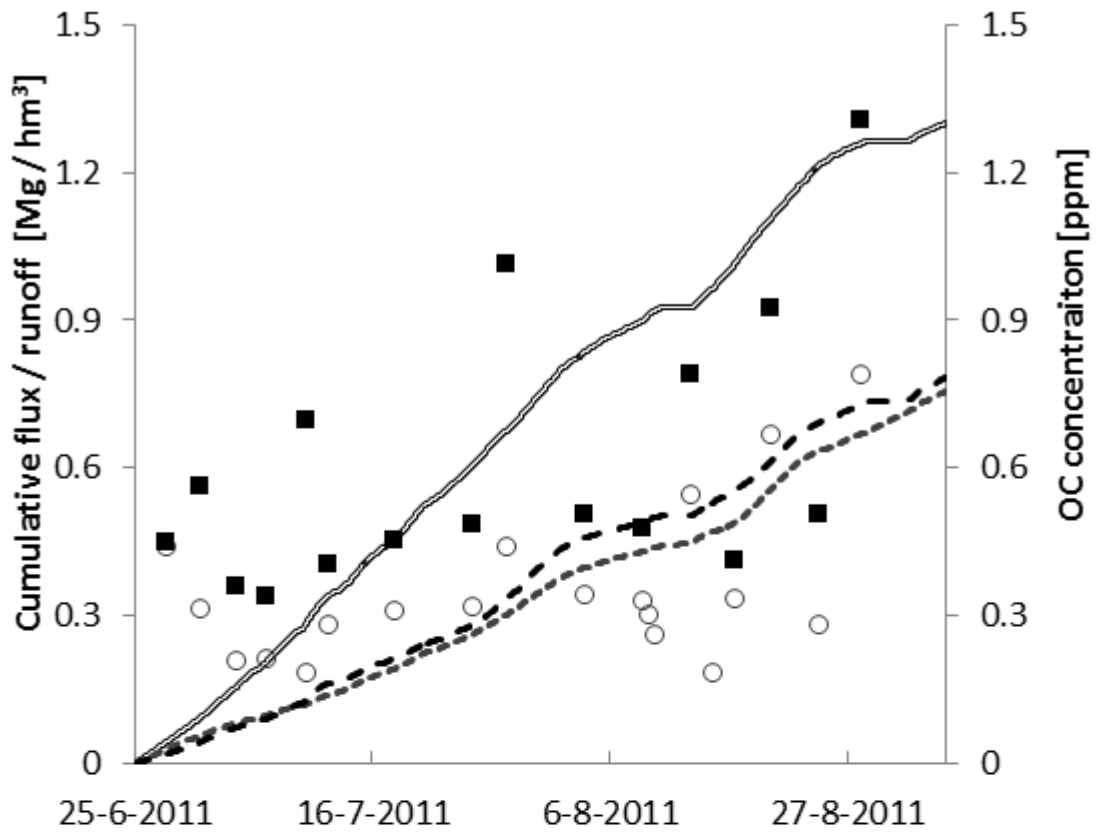
Fig. 5. Cumulative runoff and OC flux in 2011 (top) and 2012 (bottom), complemented with the OC concentrations measured at the glacier snout.
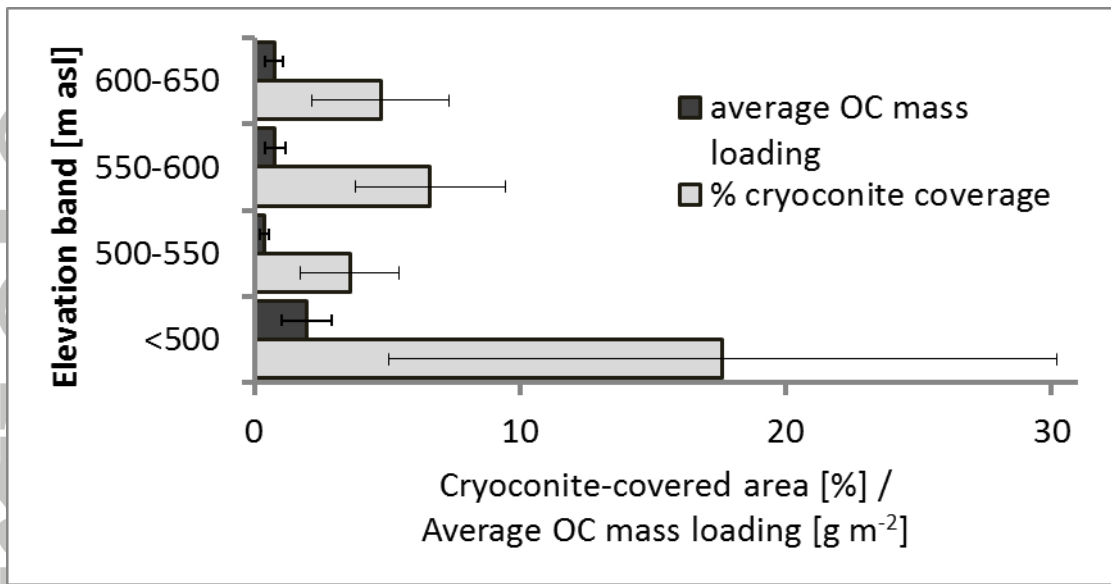
Fig. 6. Cryoconite surface coverage in 50 m elevation bands of Foxfonna glacier, and the supraglacial storage of OC in these zones (as surveyed on 25th August 2011). Error bars as 1 SD (spatial variability).
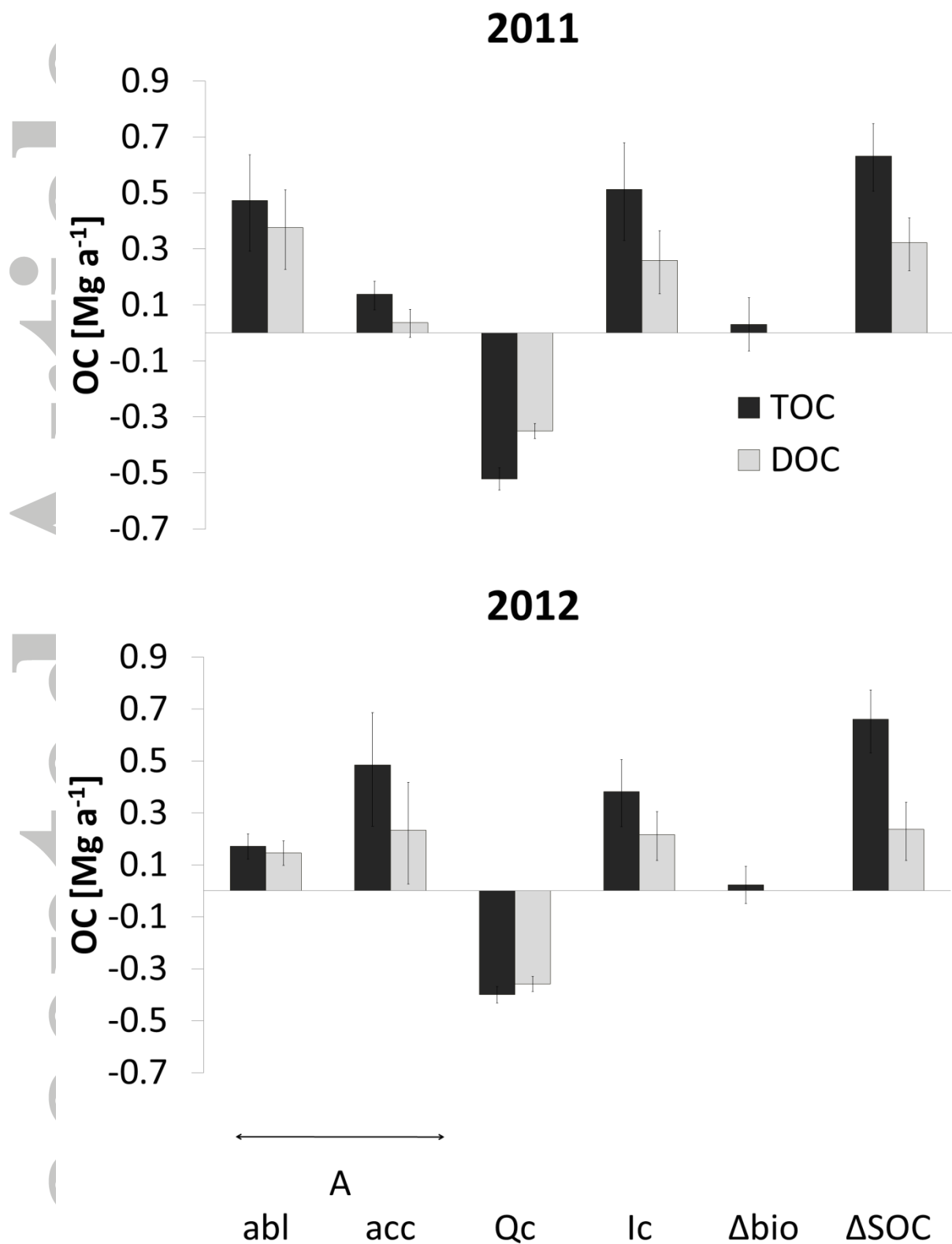
Fig. 7. Organic carbon fluxes of Foxfonna glacier for 2011 and 2012. Abbreviations: see Equations 1 and 2: abl = A^{abl}, acc = A^{acc}.